# WAVELET TRANSFORM IN CLASSIFICATION OF BIOMEDICAL IMAGES

A. Procházka* and A. Gavlasová*

* Prague Institute of Chemical Technology/Department of Computing and Control Engineering, Technická 1905, 166 28 Prague 6, Czech Republic

A.Prochazka@ieee.org, Andrea.Gavlasova@vscht.cz

**Abstract: Segmentation and texture analysis form a very important topic of the interdisciplinary area of image processing with many different applications. The paper presents selected methods of image feature extraction using both Radon and Wavelet transforms to evaluate features invariant to image rotation and translation. Features classification is then achieved by self-organizing neural networks. The paper presents (i) how image preprocessing and enhancement can simplify image segmentation, and (ii) how image segments textures can allow image areas classification. Proposed methods have been verified for simulated structures and then used for analysis of biomedical magnetic resonance images of the brain.**

## Introduction

Basic problems of digital image processing include image de-noising, enhancement, restoration of its corrupted components [9, 12, 3, 10] and segmentation. An example of this process applied to biomedical image processing is presented in Fig. 1. Problems of image segmentation are presented in the initial part of the paper.

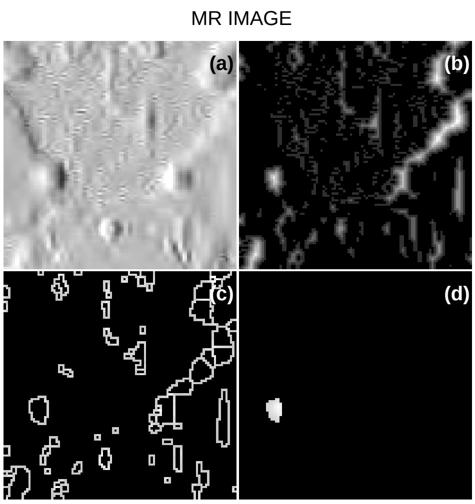


Figure 1: An example of MR image segmentation presenting **(a)** enhanced original MR area, **(b)** distance image transform, **(c)** ridge lines resulting from watershed segmentation, and **(d)** a selected segment

The main part of the paper is devoted to image components analysis and to extraction of their features. In this connection problems of image features invariant to image components rotation and translation are studied using both Radon and Wavelet transforms [11, 5, 14]. Resulting algorithms are verified both for simulated and real magnetic resonance images.

The proposed method is then followed by image components classification and class boundary estimation using self-organizing neural networks.

## Image Components Segmentation

Image segmentation methods studied in the paper consist of distance and watershed transform application followed by image ridge lines estimation. Image components features are then evaluated from their boundary signals as well as texture structures.

Segmentation [8, 4] represents an important initial step of image processing. The proposed algorithm consists of these steps

- image thresholding to convert it to the black and white form
- distance and watershed transform use to find image ridge lines presented
- extraction of a segment, its boundary signal and its texture

The process of classification assumes further the definition of a pattern matrix containing features of separate image segments. Many possibilities of their extraction [12] include

- analysis of image boundary signal or the texture inside its area
- analysis of statistical properties of the boundary signal or segment structure
- transform of boundary signal or segment structure allowing its translation and rotation independence using appropriate transforms

Proposed methods of image segmentation have been applied to selected MR images presented in Fig 1 with a chosen boundary signal given in Fig. 2.

## Image Features Extraction

To define image features independent to image segments rotation and translation it is useful to apply Radon and wavelet transforms as the fundamental tools used in

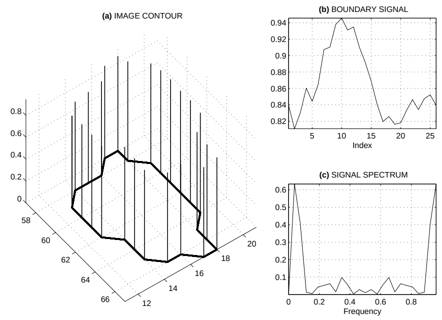


Figure 2: Selected MR image segment analysis showing its boundary signal **(a)** in three and **(b)** in two dimensions followed by **(c)** its discrete Fourier transform

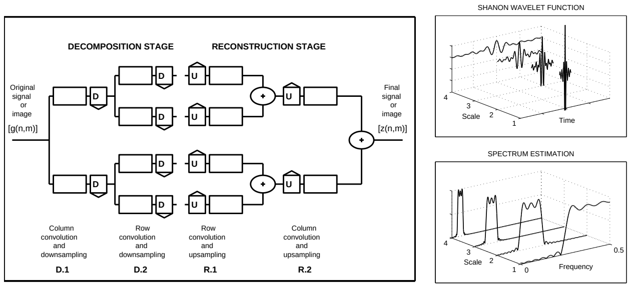


Figure 3: Wavelet transform use in signal decomposition and the effect of Shannon wavelet function dilation to its spectrum compression

the proposed approach [2, 1]. We apply this tools to simulated image, which consists of same segments. Image segments classification is in this case useless, because all segments have same features. Using rotation-invariant texture-analysis technique is showed on example of already mentioned simulated image.

*Radon Transform*

Radon transform forming a very important mathematical tool used in tomography is based upon works of Johann Radon born in 1887 Litoměřice. His doctoral dissertation has been defended in Vienna in 1910 and his most appreciated works were devoted to integral geometry. The Radon transform [6, 1] belonging to this category introduced in 1917 is defined as a collection of 1D projections around an object at angle intervals $\Theta$. The Radon transform of a two-dimensional (2-D) function $f(x,y)$ is defined as

$$R(r,\Theta)[f(x,y)] = \int_{-\infty}^{+\infty}\int_{-\infty}^{+\infty} f(x,y)\delta(r - x\cos\Theta - y\sin\Theta)\,dx\,dy \tag{1}$$

where $r$ is the perpendicular distance of a line from the origin and $\Theta$ is the angle formed by the distance vector.

A discrete Radon transform called Hough transform has been introduced in 1972 by R. Duda and P. Hart [13] as a tool for image features extraction.

*Image Wavelet Decomposition*

Signal wavelet decomposition using Discrete Wavelet Transform (DWT) provides an alternative to the Discrete Fourier Transform (DFT) for signal analysis resulting in signal decomposition into two-dimensional functions of time and scale. The main benefit of DWT over DFT is in its multi-resolution time-scale analysis ability.

Wavelet functions used for signal analysis are derived from the initial function $W(t)$ forming basis for the set of functions

$$W_{m,k}(t) = \frac{1}{\sqrt{a}}\, W\,(\frac{1}{a}\,(t-b)) \tag{2}$$

for discrete parameters of dilation $a = 2^m$ and translation $b = k\,2^m$. Wavelet dilation, which is closely related to spectrum compression, enables local and global signal analysis. The principle of signal and image decomposition and reconstruction for resolution enhancement is presented in Fig. 3.

*The decomposition stage* includes the processing of the image matrix by columns at first using wavelet (high-pass) and scaling (low-pass) function followed by row downsampling by factor $D$ in stage $D.1$. To study this problem let us denote a selected column of the image matrix $[g(n,m)]_{N,M}$ as signal $\{x(n)\}_{n=0}^{N-1} = [x(0), x(1), ..., x(N-1)]^T$. This signal can be analyzed by a half-band low-pass filter with its impulse response

$$\{s(n)\}_{n=0}^{L-1} = [s(0), s(1), \cdots, s(L-1)] \tag{3}$$

and complementary high-pass filter having impulse response

$$\{w(n)\}_{n=0}^{L-1} = [w(0), w(1), \cdots, w(L-1)] \tag{4}$$

The first stage assumes the convolution of a given signal and the appropriate filter for decomposition at first by relations

$$xl(n) = \sum_{k=0}^{L-1} s(k)x(n-k) \qquad xh(n) = \sum_{k=0}^{L-1} w(k)x(n-k) \tag{5}$$

for all values of $n$ followed by subsampling by factor $D$. In the following decomposition stage $D.2$ the same process is applied to rows of the image matrix followed by row downsampling. The decomposition stage results in this way in four images representing all combinations of low-pass and high-pass initial image matrix processing.

*The reconstruction stage* includes row upsampling by factor $U$ at first and row convolution in stage $R.1$. The corresponding images are then summed. The final step $R.2$ assumes column upsampling and convolution with reconstruction filters followed by summation of the results again. In the case of one-dimensional signal processing, steps $D.2$ and $R.1$ are omitted.

*Proposed Method*

In this section, the rotation-invariant texture-analysis technique using Radon and wavelet transforms is introduced. This technique is depicted in Fig. 4.

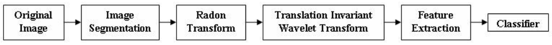


Figure 4: Block diagram of the proposed technique

The illustration shows the procedure of proposed method in block diagram. At first we identify all image components using distance and watershed transform. Then we obtain the Radon transform of the image segments and then use a translation-invariant wavelet transform to calculate the frequency components and extra the corresponding features. Rotation of the input im age corresponds to the translation of the Radon transfori along Θ. Fig. 5 shows how the Radon transform change as the simulated image rotates. The figure presents rot tion of the simulated image, whose whole the image con ponents are same, corresponds to a circular shift along Θ. Therefore, using a translation-invariant wavelet transform along Θ, we can produce rotation-invariant features.

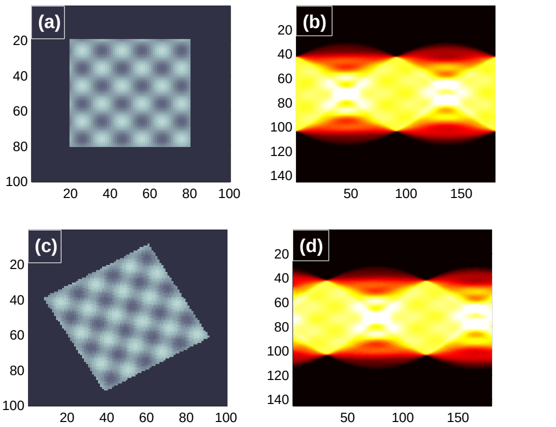


Figure 5: **(a)** Simulated image sample and **(b)** its Radon transform. **(c)** Rotated simulated image by angle $\Theta = 30^\circ$ and **(d)** its Radon transform. The translation effect is a translation along Θ (horizontal axis here)

## Results

The main goal of this paper is to show, how is the features' standard deviation changing by use different transforms by image rotation. Our wish is to have the same image features independently of image rotation. Fig. **??** presents, how passes the features analysis of simulated image, which rotates by angle from $\Theta = 0^\circ$ to $\Theta = 180^\circ$ with step $\Theta = 10^\circ$. We can distinguish mere eye, how is the variance of features and determine best method. Characteristic image features, shown in Table. 1 are computed of the sum of squared diagonal DWT transform coefficients in the first and the second decomposition levels rotated image by angle $\Theta = 10^\circ$ and they are shown in figure as a colored dots. The dots in the figure, presenting features, are evaluated **(a)** by direct application of the wavelet transform(DWT) to the rotated simulated image, **(b)** by the DWT applied to the Radon transform(RT) of rotated image and **(c)** by the wavelet transform applied to the Radon transform image of preprocessed image(Pre). Image preprocessing is performed on application of the wavelet transform followed by the thresholding. This technique is useful for image denoising, image enhancement or improving image resolution.

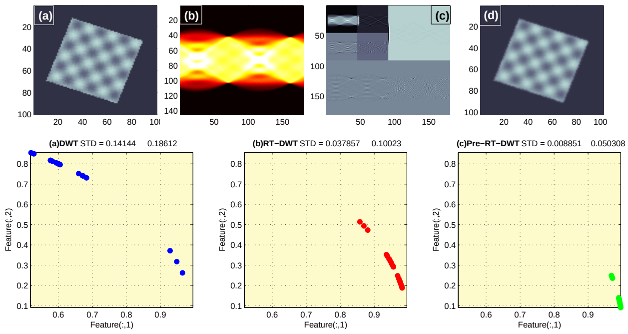


Figure 6: Figure presents **(a)** rotation of simulated image, **(b)** its Radon transform, **(c)** decomposition of the Radon transform image into 2. level, **(d)** inverse Radon transform of **(b)** and below comparison of image features evaluated by methods mentioned in text before

Table 1: Comparison of features evaluated for rotated simulated image presenting column F1 as a sum of squared diagonal DWT coefficients in the first decomposition level and column F2 as a sum of squared coeff. in the second decomp. level, for 3 different techniques (i) DWT, (ii) RT-DWT and (iii) Pre-RT-DWT

| Features of Simulated Image | | | | | | |
|---|---|---|---|---|---|---|
| | DWT | | **RT-DWT** | | **Pre-RT-DWT** | |
| **Angle** | F1 | F2 | F1 | F2 | F1 | F2 |
| 0° | 0.9284 | 0.3716 | 0.8577 | 0.5141 | 0.9706 | 0.2408 |
| 10° | 0.6029 | 0.7978 | 0.9687 | 0.2482 | 0.9928 | 0.1198 |
| 20° | 0.5278 | 0.8494 | 0.9447 | 0.3280 | 0.9946 | 0.1034 |
| 30° | 0.6021 | 0.7984 | 0.9477 | 0.3192 | 0.9956 | 0.0936 |
| 40° | 0.6595 | 0.7517 | 0.9787 | 0.2053 | 0.9915 | 0.1304 |
| 50° | 0.6724 | 0.7402 | 0.9748 | 0.2230 | 0.9902 | 0.1394 |
| 60° | 0.5994 | 0.8004 | 0.9507 | 0.3102 | 0.9945 | 0.1052 |
| 70° | 0.5193 | 0.8546 | 0.9384 | 0.3455 | 0.9947 | 0.1025 |
| 80° | 0.6050 | 0.7962 | 0.9724 | 0.2334 | 0.9920 | 0.1260 |
| 90° | 0.9482 | 0.3177 | 0.8694 | 0.4940 | 0.9685 | 0.2489 |
| 100° | 0.5770 | 0.8168 | 0.9761 | 0.2172 | 0.9928 | 0.1196 |
| 110° | 0.5179 | 0.8555 | 0.9358 | 0.3524 | 0.9951 | 0.0988 |
| 120° | 0.5935 | 0.8048 | 0.9564 | 0.2920 | 0.9958 | 0.0914 |
| 130° | 0.6706 | 0.7418 | 0.9812 | 0.1929 | 0.9911 | 0.1332 |
| 140° | 0.6827 | 0.7307 | 0.9821 | 0.1882 | 0.9907 | 0.1358 |
| 150° | 0.5822 | 0.8131 | 0.9549 | 0.2970 | 0.9948 | 0.1015 |
| 160° | 0.5264 | 0.8502 | 0.9434 | 0.3316 | 0.9948 | 0.1022 |
| 170° | 0.5765 | 0.8171 | 0.9771 | 0.2129 | 0.9937 | 0.1119 |
| 180° | 0.9650 | 0.2623 | 0.8808 | 0.4734 | 0.9717 | 0.2361 |

Table 2: Comparison of standard deviation(STD) of the sum of squared diagonal DWT transform coefficients in the first and the second decomposition levels using images obtained by rotation from 0 to 180 degrees with step 10° using these techniques (i) the plain DWT (ii) application of the Radon transform(RT) followed by DWT and (iii) using the Radon transform(RT) on preprocessed image(Pre) followed by DWT

| STD of Simulated Image Features | | |
|---|---|---|
| | Feature-1 | Feature-2 |
| DWT | 0.1414 | 0.1861 |
| RT-DWT | 0.0379 | 0.1002 |
| Pre-RT-DWT | 0.0089 | 0.0503 |

Table 3: Comparison of standard deviation(STD) of the sum of squared diagonal DWT transform coefficients in the first and the second decomposition levels using images obtained by rotation from 0 to 180 degrees with step 10° using these techniques (i) the plain DWT (ii) application of the Radon transform(RT) followed by DWT and (iii) using the Radon transform(RT) on preprocessed image(Pre) followed by DWT

| STD of MR Image Features | | |
|---|---|---|
| | Feature-1 | Feature-2 |
| DWT | 0.0013 | 0.0254 |
| RT-DWT | $2.97 \cdot 10^{-5}$ | 0.0023 |
| Pre-RT-DWT | $1.4 \cdot 10^{-5}$ | 0.0016 |

## Conclusion

The proposed technique was applied also to MR image. Because of the difficulty of application of segmentation process we omit this block. Rotation has been applied to whole MR image and features are obtained by using wavelet and Radon transform and image preprocessing. Example of rotated MR image and obtaining features presents Fig. 7.

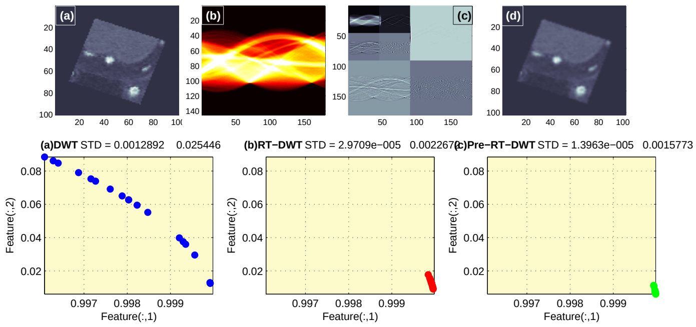


Figure 7: Figure presents proposed technique applied on MR image

Apparently on Fig. 6, 7, recommended connection of Radon and wavelet transform dramatically keep down the feature variance influenced by image rotation. If we yet add image preprocessing, results get better visible. Except visual comparison are concrete numerical results, which bear to effectivity of proposed method, introduced in Table. 2, 3.

## Acknowledgments


The work has been supported by the research grant of the Faculty of Chemical Engineering of the Institute of Chemical Technology, Prague No. MSM 6046137306.


## References


[1] http://en.wikipedia.org/wiki/radon_transform. Internet Encyklopedia, 7 2005. 84.226.54.188.

[2] http://www-stat.stanford.edu/~jstarck/. The Curvelet Home Page, 2005.

[3] A. Procházka and A. Gavlasová and K. Volka. Wavelet Transform in Image Recognition. In *International conference ELMAR05, Zadar. Croatia*. IEEE, 2005.

[4] S. Arivazhagan and L. Ganesan. Texture Segmentation Using Wavelet Transform. *Pattern Recogn. Lett.*, 24(16):3197–3203, 2003.

[5] S. Arivazhagan and L. Ganesan. Automatic Target Detection Using Wavelet Transform. *Eurasip Journal on Applied Sig. Proc.*, 17:2663–2674, 2004.

[6] R. N. Bracewell. *Fourier Analysis and Imaging*. Kluwer Academic Press, 2003.

[7] D. I. Choi and S. H. Park. Self-Creating and Organizing Neural Networks. *IEEE Trans. Neural Networks*, 5(4):561–575, July 1994.

[8] R. C. Gonzales, R. E. Woods, and S. L. Eddins. *Digital Image Processing Using MATLAB*. Prentice Hall, 2004.

[9] Onur G. Guleryuz. Iterated Denoising for Image Recovery. In *Data Compression Conference (DCC '02), Snao Bird, Utah*. IEEE, 2002.

[10] J. L. Starck and E. Candes and D.L. Donoho. The Curvelet Transform for Image Denoising. *IEEE Trans. on Image processing*, 11(6):670–684, 2002.

[11] K. Jafari-Khouzani and H. Soltanian-Zadeh. Rotation-Invariant Multiresolution Texture Analysis Using Radon and Wavelet Transforms. *IEEE Trans. on Image processing*, 14(6):783–795, 2005.

[12] M. Nixon and A. Aguado. *Feature Extraction & Image Processing*. NewNes Elsevier, 2004.

[13] R. O. Duda and P. E. Hart. Use of the Hough Transformation to Detect Lines and Curves in Pictures. *Comm. ACM*, 15(1):11–15, 1972.

[14] P. Toft. *The Radon Transform - Theory and Implementation*. PhD thesis, Technical University of Denmark, 1996.